Information content for observations of forest carbon stocks and fluxes when assimilated with the DALEC carbon balance model

E. Pinnington

October 22, 2014

1 Introduction

A large amount of data is currently being gathered that is relevant to the carbon balance of forests, with much of this data coming from Eddy covariance flux towers [1]. Attempts are also being made to combine this data with models of forest carbon stocks and fluxes, such as the Data Assimilation Linked Ecosystem Carbon model (DALEC) [11], in a data assimilation scheme. Currently, however, there are limitations with such schemes as there is a lack of understanding about the additional information provided by different observations. Better understanding of the information content of carbon balance observations will help inform measurement campaigns of when and which observations to take in order to gain the most possible information about the system. In this report we will look at different information content measures which have been used in meteorological data assimilation [4, 8, 9] and apply these to carbon balance observations assimilated with DALEC. We begin by introducing the DALEC model which will initially be used to look at the information content in different observations.

2 The DALEC Model

The DALEC model is a simple process-based model describing the carbon balance of an evergreen forest ecosystem [11]. The model is constructed of five carbon pools (foliage (C_f), fine roots (C_r), woody stems and coarse roots (C_w), fresh leaf and fine root litter (C_l) and soil organic matter and coarse woody debris (C_s)) linked via fluxes. The gross primary production function (GPP) uses meteorological driving data and the site's leaf area index (a function of C_f) to calculate the total amount of carbon to be allocated at a daily time step.

The model equations for the carbon pools at day $t+1$ are as follows:

$$C_f(t+1) = (1-p_5)C_f(t) + p_3(1-p_2)GPP(C_f(t),\phi), \tag{1}$$
$$C_r(t+1) = (1-p_7)C_r(t) + p_4(1-p_3)(1-p_2)GPP(C_f(t),\phi), \tag{2}$$
$$C_w(t+1) = (1-p_6)C_w(t) + (1-p_4)(1-p_3)(1-p_2)GPP(C_f(t),\phi), \tag{3}$$
$$C_l(t+1) = (1-(p_1+p_8)T(t))C_l(t) + p_5C_f(t) + p_7C_r(t), \tag{4}$$
$$C_s(t+1) = (1-p_9T(t))C_s + p_6C_w(t) + p_1T(t)C_l(t), \tag{5}$$

where $T(t) = \frac{1}{2}exp(p_{10}T_m(t))$, T_m is daily mean temperature, $p_1, \dots, p_{10}$ are rate parameters and ϕ represents the meteorological driving data used in the GPP function. The full details of this version of DALEC can be found in [11]. We now introduce Shannon Information Content as one method to assess the information content in different carbon balance observations.

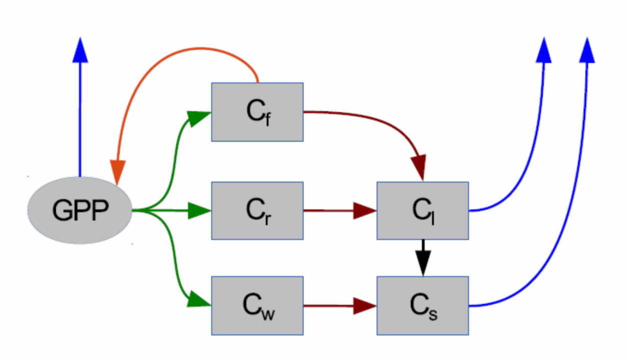

Figure 1: Representation of the carbon fluxes in the DALEC carbon balance model. Green arrows represent C allocation, dark red and black arrows represent litterfall and decomposition fluxes, blue arrows represent respiration fluxes and the light red arrow represents the feedback of foliar carbon to the GPP function. [2]

3 Introduction to Variational Assimilation

3.1 Baye's Theorem and 3D-Var

3.2 4D-Var

4 Information Content Measures

Information content measures are already being used to quantify the different levels of information provided by observations in the development of satellite instruments [3, 10] and in operational data assimilation schemes [4, 9]. In these fields two of the more widely used measures are Shannon Information Content (also known as entropy reduction) and the degrees of freedom for signal. We will apply both methods for observations assimilated with DALEC.

4.1 Shannon Information Content

In DA Shannon Information Content (SIC) is a measure of the reduction in entropy given a set of observations. Entropy physically corresponds to the volume in state space taken up by the probability density function (*pdf*) describing the knowledge of the state. When a measurement is made the volume of this *pdf* decreases, the information content of the measurement is a measure of the factor by which it decreases [8]. If $P_b(x)$ is our knowledge of the state before an observation and $P_o(x|y)$ is our knowledge after an observation then we have entropies,

$$S[P_b(x)] = -\int P_b(x)\log_2[P_b(x)]dx \quad \text{and} \quad S[P_o(x|y)] = -\int P_o(x|y)\log_2[P_o(x|y)]dx.$$

The entropy reduction, or SIC, due to the observation is then,

$$SIC = S[P_b(x)] - S[P_o(x|y)]. \tag{6}$$

If we assume all *pdfs* are Gaussian and use the natural logarithm as opposed to $\log_2$ (for algebraic convenience) [8] the entropy of a multivariate Gaussian distruibution for a vector $\underline{x}$ with n elements (before and after observations) can be derived as,

$$S[P_b(\underline{x})] = n\ln(2\pi e)^{\frac{1}{2}} + \frac{1}{2}\ln|\mathbf{B}| \tag{7}$$

and

$$S[P_o(\underline{x}|\underline{y})] = n\ln(2\pi e)^{\frac{1}{2}} + \frac{1}{2}\ln|\mathbf{A}| \tag{8}$$

where $\mathbf{B}$ is the background error covariance matrix and $\mathbf{A}$ is the analysis error covariance matrix. Combining equations 6, 7 and 8 we can write the SIC as,

$$SIC = \frac{1}{2}\ln\frac{|\mathbf{B}|}{|\mathbf{A}|}. \tag{9}$$

4.2 Degrees of Freedom for Signal

The degrees of freedom for signal (DFS) indicates the number of elements of the state that have been measured by the observations. If we consider a state vector $\underline{x}$ with n elements (or n degrees of freedom) then the maximum value the DFS could obtain would be n, in this case all elements of the state would have been measured. Conversely if $DFS = 0$ then no elements of the state would have been measured by our observations [6].

We have background and analysis error covariance matrices $\mathbf{B}$ and $\mathbf{A}$, the eigenvalues of each matrix gives a representation for the uncertainty in the direction of the associated eigenvector, thus by comparing the eigenvalues of both matrices we can determine the reduction in uncertainty given a set of observations [10].

In order to do this we take $\mathbf{B}^{\frac{-1}{2}}$ such that $\mathbf{B}^{-1} = \mathbf{B}^{\frac{-1}{2}}\mathbf{B}^{\frac{-1}{2}}$. We now take $\mathbf{Q}$ to be the orthogonal matrix composed of the eigenvectors of $\mathbf{B}^{\frac{-1}{2}}\mathbf{A}\mathbf{B}^{\frac{-1}{2}}$ we have,

$$\mathbf{Q}^T\left(\mathbf{B}^{\frac{-1}{2}}\mathbf{A}\mathbf{B}^{\frac{-1}{2}}\right)\mathbf{Q} = \mathbf{\Lambda}, \tag{10}$$

$$\mathbf{Q}^T\left(\mathbf{B}^{\frac{-1}{2}}\mathbf{B}\mathbf{B}^{\frac{-1}{2}}\right)\mathbf{Q} = \mathbf{I}_{nxn} \tag{11}$$

where $\mathbf{\Lambda}$ is a diagonal matrix. Each diagonal element of our transformed $\mathbf{B}$ is equal to one and corresponds to one degree of freedom. The diagonal elements of $\mathbf{\Lambda}$ correspond to the matrixs eigenvalues and can be interpreted as the relative reduction in variance for each of the n degrees of freedom [9]. We can then define the DFS as,

$$\begin{aligned} DFS &= \text{trace}(\mathbf{I}_{nxn} - \mathbf{\Lambda}) \\ &= n - \text{trace}(\mathbf{\Lambda}) \\ &= n - \text{trace}(\mathbf{B}^{\frac{-1}{2}}\mathbf{A}\mathbf{B}^{\frac{-1}{2}}) \\ &= n - \text{trace}(\mathbf{B}^{-1}\mathbf{A}). \end{aligned} \tag{12}$$

5 Shannon Information Content for DALEC

We begin by using SIC to understand the information content for different observations at one time when being assimilated with the DALEC model. We specify the state vector for the assimilation as,

$$\underline{x}_b = (C_f, C_r, C_w, C_l, C_s)^T,$$

where the elements of the state vector have variances, $\sigma^2_{cf,b}, \dots, \sigma^2_{cs,b}$, respectively. We then have the following background error covariance matrix,

$$\mathbf{B} = \begin{pmatrix} \sigma^2_{cf,b} & 0 & 0 & 0 & 0 \\ 0 & \sigma^2_{cr,b} & 0 & 0 & 0 \\ 0 & 0 & \sigma^2_{cw,b} & 0 & 0 \\ 0 & 0 & 0 & \sigma^2_{cl,b} & 0 \\ 0 & 0 & 0 & 0 & \sigma^2_{cs,b} \end{pmatrix},$$

here we assume a diagonal background error covariance matrix. In order to calculate the SIC we need $\left|\mathbf{A}^{-1}\right|$ we have,

$$\mathbf{A}^{-1} = \mathbf{J}'' = \mathbf{B}^{-1} + \mathbf{H}^T\mathbf{R}^{-1}\mathbf{H},$$

where $\mathbf{J}''$ is the Hessian of $\mathbf{J}$, the cost function to be minimized in Three-Dimensional Variational Data Assimilation (3D-Var), and $\mathbf{H}$ is the linearized observation operator.

5.1 SIC for a single observation at one time

If we first consider one observation of C_f (the first element of our state vector $\underline{x}$) an analytical expression for the SIC can be derived using,

$$\mathbf{H}_0 = \begin{pmatrix} 1 & 0 & 0 & 0 & 0 \end{pmatrix},$$

where $\mathbf{H}_0 = \frac{\delta C_f(t_0)}{\delta \underline{x}}$ is the linearized observation operator at time t_0. As we have a single observation at one time our observation error covariance matrix, $\mathbf{R}$, is just the variance of our observation of C_f, $\sigma^2_{cf,o}$, at time t_0. Therefore,

$$\mathbf{R} = \sigma^2_{cf,o}$$

and

$$\begin{aligned} \mathbf{J}'' &= \mathbf{B}^{-1} + \mathbf{H}^T\mathbf{R}^{-1}\mathbf{H} \\ &= \begin{pmatrix} \sigma^{-2}_{cf,b} + \sigma^{-2}_{cf,o} & 0 & 0 & 0 & 0 \\ 0 & \sigma^{-2}_{cr,b} & 0 & 0 & 0 \\ 0 & 0 & \sigma^{-2}_{cw,b} & 0 & 0 \\ 0 & 0 & 0 & \sigma^{-2}_{cl,b} & 0 \\ 0 & 0 & 0 & 0 & \sigma^{-2}_{cs,b} \end{pmatrix}. \end{aligned}$$

We then have,

$$SIC = \frac{1}{2} ln \frac{|\mathbf{B}|}{|\mathbf{A}|} = \frac{1}{2} ln \left|\mathbf{B}\right| \left|\mathbf{J}''\right|.$$

Hence,

$$SIC = \frac{1}{2} ln \frac{(\sigma^2_{cf,o} + \sigma^2_{cf,b})}{\sigma^2_{cf,o}} = \frac{1}{2} ln \left(1 + \frac{\sigma^2_{cf,b}}{\sigma^2_{cf,o}}\right).$$

Here we see the SIC is dependant on the ratio between the two variances and this will be the same for all other carbon pool observations. Something about better depending on pool observed.

One of the main observations made of the carbon balance of a forest at flux tower sites is the net ecosystem exchange (NEE) of CO$_2$, which can be estimated by DALEC as the difference between GPP and the respiration of C_l and C_s, giving,

$$NEE(t) = -(1 - p_2)GPP(C_f(t), \phi) + p_8 C_l T(t) + p_9 C_s T(t).$$

For a single observation of NEE at one time, t_0, an analytical expression for the SIC can be derived using,

$$\mathbf{H}_0 = \begin{pmatrix} -(1-p_2)\zeta_0 & 0 & 0 & p_8 T_0 & p_9 T_0 \end{pmatrix},$$

where $\zeta_0 = GPP'(C_f(t_0), \phi)$, $T_0 = T(t_0)$ and $\mathbf{H}_0 = \frac{\delta NEE(t_0)}{\delta \underline{x}}$ is the linearized observation operator at time t_0. Again our observation error covariance matrix, $\mathbf{R}$, is just the variance of our observation of NEE, $\sigma_{nee,0}^2$, at time t_0. Therefore,

$$\mathbf{R} = \sigma_{nee,0}^2$$

and

$$\begin{aligned} \mathbf{J}'' &= \mathbf{B}^{-1} + \mathbf{H}^T \mathbf{R}^{-1} \mathbf{H} \\ &= \begin{pmatrix} \sigma_{cf,b}^{-2} + \sigma_{nee,0}^{-2}(1-p_2)^2\zeta_0^2 & 0 & 0 & \sigma_{nee,0}^{-2}(1-p_2)\zeta_0 p_8 T_0 & \sigma_{nee,0}^{-2}(1-p_2)\zeta_0 p_9 T_0 \\ 0 & \sigma_{cr,b}^{-2} & 0 & 0 & 0 \\ 0 & 0 & \sigma_{cw,b}^{-2} & 0 & 0 \\ \sigma_{nee,0}^{-2}(1-p_2)\zeta_0 p_8 T_0 & 0 & 0 & \sigma_{cl,b}^{-2} + \sigma_{nee,0}^{-2} p_8^2 T_0^2 & \sigma_{nee,0}^{-2} p_8 p_9 T_0^2 \\ \sigma_{nee,0}^{-2}(1-p_2)\zeta_0 p_9 T_0 & 0 & 0 & \sigma_{nee,0}^{-2} p_8 p_9 T_0^2 & \sigma_{cs,b}^{-2} + \sigma_{nee,0}^{-2} p_9^2 T_0^2 \end{pmatrix}. \end{aligned}$$

We then have,

$$SIC = \frac{1}{2} ln \frac{|\mathbf{B}|}{|\mathbf{A}|} = \frac{1}{2} ln \, |\mathbf{B}| \, |\mathbf{J}''| \, .$$

Hence,

$$SIC = \frac{1}{2} ln \frac{(p_2 - 1)^2 \zeta_0^2 \sigma_{cf,b}^2 + \sigma_{nee,0}^2 + T_0^2 (p_9^2 \sigma_{cs,b}^2 + p_8^2 \sigma_{cl,b}^2)}{\sigma_{nee,0}^2}.$$

If we assume that the variances and parameters here are fixed we can see that the size of the SIC is dependent on the temperature term, T_0, and the square of the first derivative of GPP, ζ_0^2. Generally, the value of GPP (and its first derivative) is highest in summer with higher total daily irradiance and higher temperatures. We therefore have that there will be more information content in observations that are taken when temperatures are higher. ***Physically this makes sense as more NEE takes place when temperatures are higher (to a point) so measurements are of greater magnitude and give us more information of carbon fluxes***. By plotting the SIC for a single observation of NEE varying with three years of meteorological driving data and the temperature term for the same period of the same data we can see that both are closely linked in figure 2.

However the relationship is not linear as the magnitude of GPP's first derivative is also dependent on daily irradiance and the value of the foliar carbon pool (C_f). This show that observations of NEE made in the summer are much more valuable than those made in the winter assuming warmer temperatures, higher daily irradiance and a higher amount of foliar carbon in the summer.

5.2 SIC for successive observations over a time window

Following the results for SIC based at a single time, we now consider the SIC when successive observations are added over a period of time. The DALEC model is now built into a Four-Dimensional Variational Data Assimilation (4D-Var) framework where our observation operator, $\mathbf{H}$, and observation error covariance matrix, $\mathbf{R}$, are now,

$$\mathbf{H} = \begin{pmatrix} \mathbf{H}_0 \\ \mathbf{H}_1 \mathbf{M}_0 \\ \vdots \\ \mathbf{H}_n \mathbf{M}_{n,0} \end{pmatrix} \quad \text{and} \quad \mathbf{R} = \begin{pmatrix} \mathbf{R}_0 & 0 & 0 & 0 \\ 0 & \mathbf{R}_1 & 0 & 0 \\ 0 & 0 & \ddots & 0 \\ 0 & 0 & 0 & \mathbf{R}_n \end{pmatrix},$$

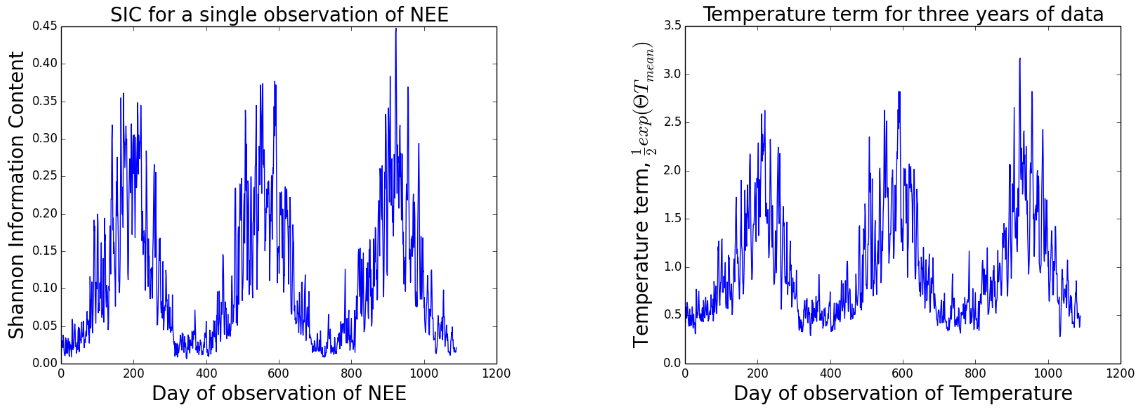

(a) SIC for a single observation of NEE.

(b) Temperature term, $\frac{1}{2}exp(\Theta T_{mean})$.

Figure 2: SIC and temperature varying over three years using driving data from Oregon pine forest.

where $\mathbf{H}_i$ is our linearized observation operator at time t_i, $\mathbf{M}_{i,0} = \mathbf{M}_{i-1}\mathbf{M}_{i-2}\cdots\mathbf{M}_0$ is our linearized model evolving the state vector, $\underline{x}_b$, at time t_0 to time t_i and $\mathbf{R}_i$ is the observation error covariance matrix corresponding to $\mathbf{H}_i$ at time t_i [7]. Firstly the tangent linear model for DALEC was calculated analytically as $\mathbf{M}_i = \frac{\delta m_i}{\delta \underline{x}_i}$.

We begin by considering successive observations of Cf in time. Here we again have,

$$\mathbf{H}_i = \begin{pmatrix} 1 & 0 & 0 & 0 & 0 \end{pmatrix} \quad \text{and} \quad \mathbf{R}_i = \sigma^2_{cf,o}.$$

The linearized model at time t_i is given as,

$$\mathbf{M}_i = \begin{pmatrix} (1-p_5)+p_3(1-p_2)GPP'(C_f(t_i),\phi) & 0 & 0 & 0 & 0 \\ p_4(1-p_3)(1-p_2)GPP'(C_f(t_i),\phi) & (1-p_7) & 0 & 0 & 0 \\ (1-p_4)(1-p_3)(1-p_2)GPP'(C_f(t_i),\phi) & 0 & (1-p_6) & 0 & 0 \\ p_5 & p_7 & 0 & (1-(p_1+p_8)T(t_i)) & 0 \\ 0 & 0 & p_6 & p_1T(t_i) & (1-p_9T(t_i)) \end{pmatrix}.$$

Then for two successive observations of Cf we have,

$$\mathbf{H} = \begin{pmatrix} \mathbf{H}_0 \\ \mathbf{H}_1\mathbf{M}_0 \end{pmatrix} = \begin{pmatrix} 1 & 0 & 0 & 0 & 0 \\ (1-p_5)+p_3(1-p_2)GPP'(C_f(t_0),\phi) & 0 & 0 & 0 & 0 \end{pmatrix}$$

and

$$\mathbf{R} = \begin{pmatrix} \mathbf{R}_0 & 0 \\ 0 & \mathbf{R}_1 \end{pmatrix} = \begin{pmatrix} \sigma^2_{cf,o} & 0 \\ 0 & \sigma^2_{cf,o} \end{pmatrix}.$$

We then have,

$$SIC = \frac{1}{2}ln\left|\mathbf{B}\right|\left|\mathbf{J}''\right| = \frac{1}{2}ln\left(1+\frac{\sigma^2_{cf,b}}{\sigma^2_{cf,o}}+\frac{\sigma^2_{cf,b}\eta_0^2}{\sigma^2_{cf,o}}\right),$$

where $\eta_i = (1-p_5)+p_3(1-p_2)GPP'(C_f(t_i),\phi)$. We can continue adding more observations at successive times and we start to see a pattern. For three observations at successive times we have,

$$SIC = \frac{1}{2}ln\left(1+\frac{\sigma^2_{cf,b}}{\sigma^2_{cf,o}}+\frac{\sigma^2_{cf,b}\eta_0^2}{\sigma^2_{cf,o}}+\frac{\sigma^2_{cf,b}\eta_0^2\eta_1^2}{\sigma^2_{cf,o}}\right),$$

for four,

$$SIC = \frac{1}{2} ln\left(1 + \frac{\sigma^2_{cf,b}}{\sigma^2_{cf,o}} + \frac{\sigma^2_{cf,b}\eta_0^2}{\sigma^2_{cf,o}} + \frac{\sigma^2_{cf,b}\eta_0^2\eta_1^2}{\sigma^2_{cf,o}} + \frac{\sigma^2_{cf,b}\eta_0^2\eta_1^2\eta_2^2}{\sigma^2_{cf,o}}\right).$$

Using a simple proof by induction we find that for n observations we have,

$$SIC \text{ for } n \text{ observations of } Cf \;= \frac{1}{2} ln\left(1 + \frac{\sigma^2_{cf,b}}{\sigma^2_{cf,o}}(1 + \sum_{k=0}^{n-2}\prod_{i=0}^{k}\eta_i^2)\right)$$

We have plotted the SIC for increasing numbers of observations of Cf using three years of meteorological driving data from an Oregan pine forest as seen in figure 3.

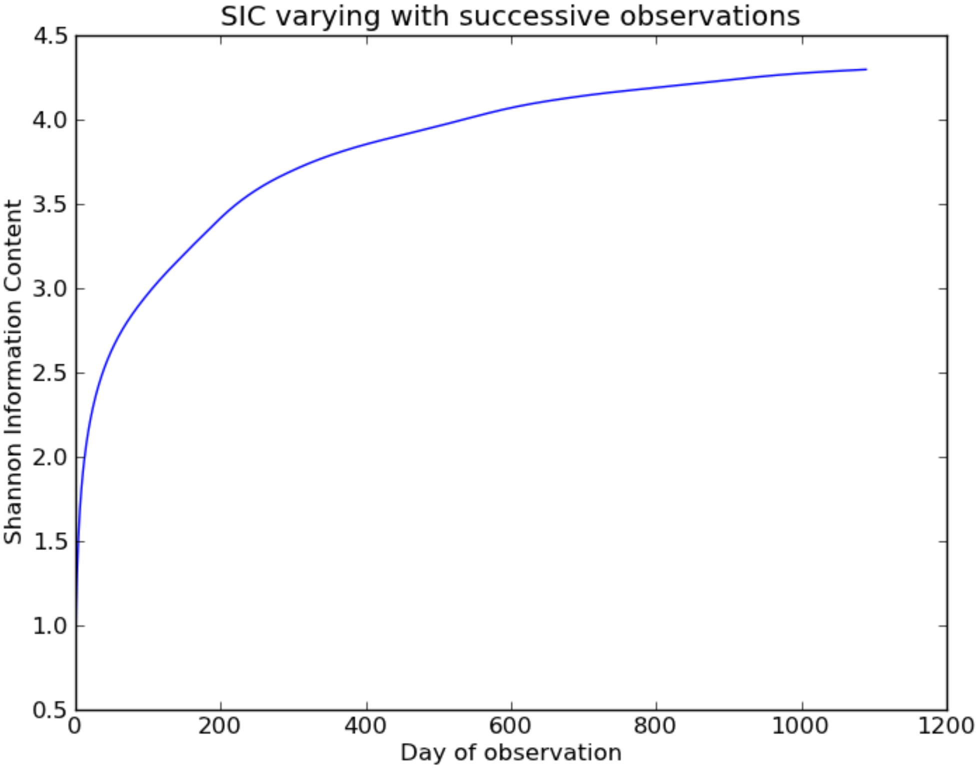

Figure 3: SIC varying as successive observations of Cf are added using driving data from Oregon pine forest.

As before with a single observation at one time we can repeat this with successive observations of NEE instead of Cf this is plotted in figure 4. Here we can see the seasonal cycle of information content as in figure 2 with little information being added during the winter months and more being added during summer.

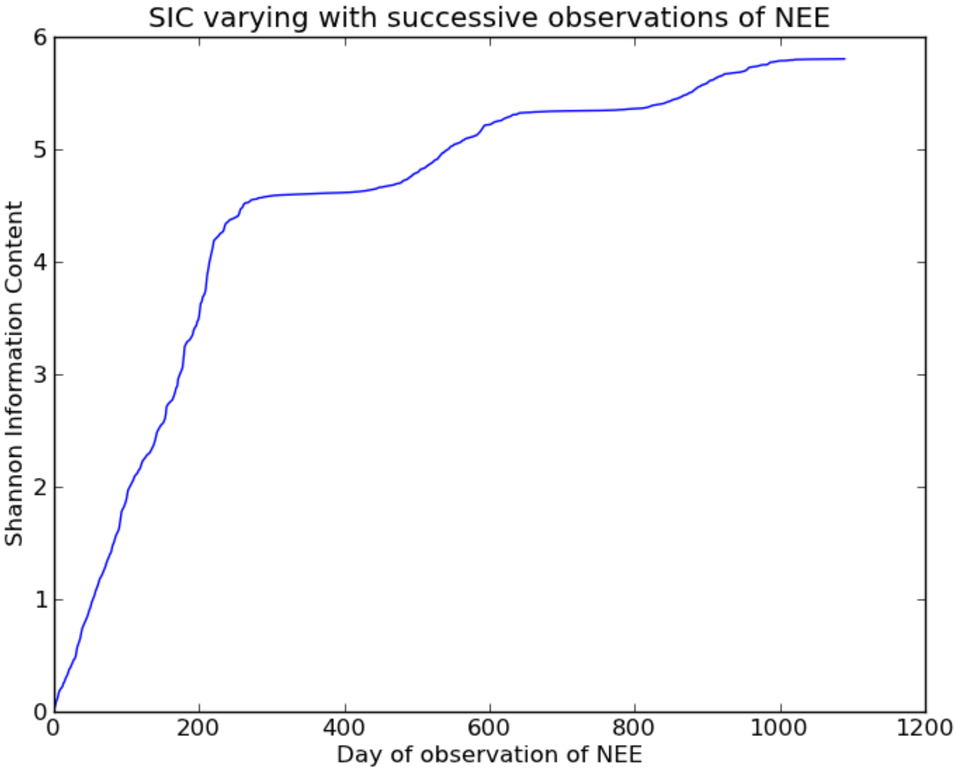

Figure 4: SIC varying as successive observations of NEE are added using driving data from Oregon pine forest.

6 Degrees of freedom for signal for DALEC

7 Conclusion

References

[1] Dennis Baldocchi. Turner review no. 15.'breathing'of the terrestrial biosphere: lessons learned from a global network of carbon dioxide flux measurement systems. *Australian Journal of Botany*, 56(1):1–26, 2008.

[2] Sylvain Delahaies, Ian Roulstone, and Nancy Nichols. A regularization of the carbon cycle data-fusion problem. In *EGU General Assembly Conference Abstracts*, volume 15, page 4087, 2013.

[3] RJ Engelen and GL Stephens. Information content of infrared satellite sounding measurements with respect to co2. *Journal of Applied Meteorology*, 43(2):373–378, 2004.

[4] Michael Fisher. *Estimation of entropy reduction and degrees of freedom for signal for large variational analysis systems*. European Centre for Medium-Range Weather Forecasts, 2003.

[5] Michael Fisher and European Centre for Medium Range Weather Forecasts. *Estimation of entropy reduction and degrees of freedom for signal for large variational analysis systems.*

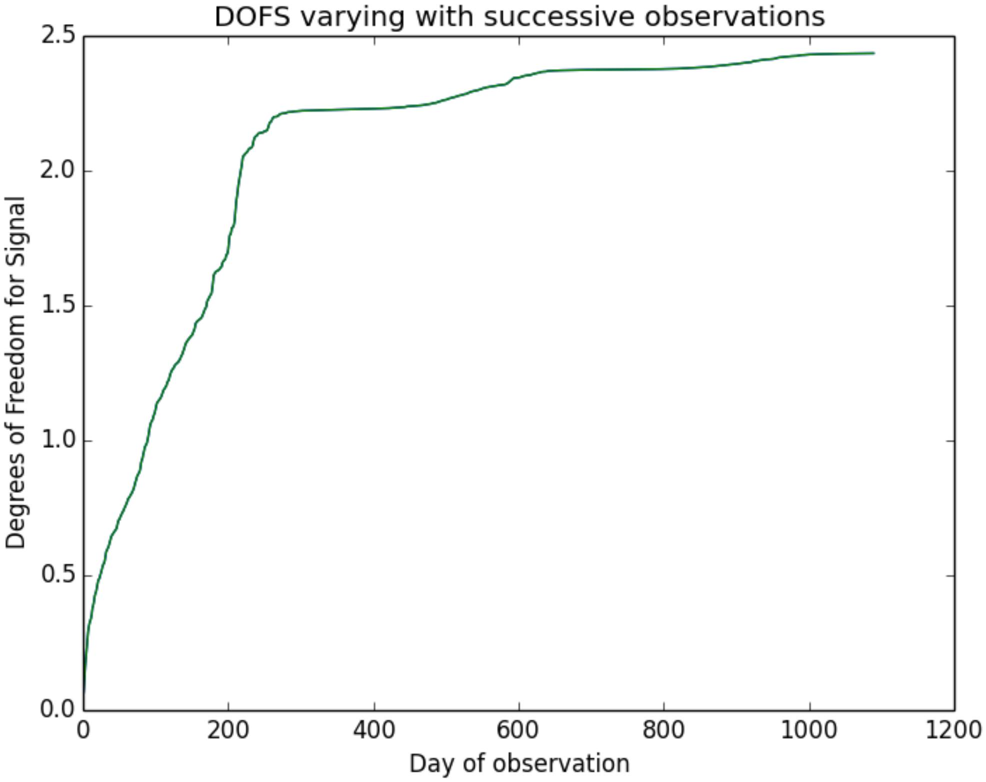

Figure 5: $DOFS$ varying as successive observations of NEE are added using driving data from Oregon pine forest.

Reading, England : European Centre for Medium-Range Weather Forecasts, 2003. Cover title.

[6] Alison Fowler and Peter Jan van Leeuwen. Measures of observation impact in gaussian data assimilation. 2011.

[7] John M Lewis, Sivaramakrishnan Lakshmivarahan, and Sudarshan Dhall. *Dynamic data assimilation: a least squares approach*, volume 13. Cambridge University Press, 2006.

[8] Clive D Rodgers et al. *Inverse methods for atmospheric sounding: Theory and practice*, volume 2. World scientific Singapore, 2000.

[9] Adrian Sandu, Kumaresh Singh, Mohamed Jardak, Kevin Bowman, and Meemong Lee. A practical method to estimate information content in the context of 4d-var data assimilation. i: Methodology. 2012.

[10] Laura M Stewart, SL Dance, and NK Nichols. Correlated observation errors in data assimilation. *International journal for numerical methods in fluids*, 56(8):1521–1527, 2008.

[11] Mathew Williams, Paul A Schwarz, Beverly E Law, James Irvine, and Meredith R Kurpius. An improved analysis of forest carbon dynamics using data assimilation. *Global Change Biology*, 11(1):89–105, 2005.